Ocean Sci. Discuss., 8, 2197–2235, 2011
www.ocean-sci-discuss.net/8/2197/2011/
doi:10.5194/osd-8-2197-2011

Ocean Science Discussions

Influence of Ross Sea Bottom Water changes on the warming and freshening of the Antarctic Bottom Water in the Australian-Antarctic Basin

K. Shimada[1], S. Aoki[1], K. I. Ohshima[1], and S. R. Rintoul[2,3,4,5]

[1]Institute of Low Temperature Science, Hokkaido University, Sapporo, Japan
[2]CSIRO Marine and Atmospheric Research, Hobart, Tasmania, Australia
[3]Centre for Australian Weather and Climate Research, Hobart, Tasmania, Australia
[4]Antarctic Climate and Ecosystems Cooperative Research Centre, Hobart, Tasmania, Australia
[5]CSIRO Wealth from Oceans National Research Flagship, Hobart, Tasmania, Australia

Received: 14 October 2011 – Accepted: 17 October 2011 – Published: 2 November 2011

Correspondence to: K. Shimada (k_shimada@lowtem.hokudai.ac.jp)

Published by Copernicus Publications on behalf of the European Geosciences Union.

Abstract

The WOCE Hydrographic Program (WHP) and repeated hydrographic data were used to document overall property changes of the Antarctic Bottom Water (AABW) in the Australian-Antarctic Basin between the 1990s and 2000s. Strong cooling and freshening is observed on isopycnals for layers denser than $\gamma^n = 28.30$. Changes in average salinity and potential temperature below this isopycnal correspond to basin-wide warming of 1300 ± 200 TW and freshening of 24 ± 3 Gt yr^{-1}. While freshening can be explained by freshening of major source waters, i.e., the High Salinity Shelf Water (HSSW) of the Ross Sea and the dense shelf water formed in the Adélie and George V Land (AGVL) region, extensive warming of the AABW cannot be explained by warming of the source waters. A possible cause of warming of the AABW is a decrease in supply of the Ross Sea Bottom Water (RSBW). Hydrographic profiles between the Drygalski Trough of the Western Ross Sea and 150° E were analyzed in the context of a simple advective-diffusive model to assess the causes of the observed changes. The RSBW has also warmed by a larger amount than its source water (the HSSW). The model suggests that the warming of the RSBW observed between the 1970s and 2000s can be explained by a 21 ± 23 % reduction in transport of the RSBW and an enhancement of the vertical diffusion of heat as a result of a 30 ± 7 % weakening of the abyssal stratification. Freshening of the HSSW reduced the salinity and density stratification between the bottom water layer and overlying ambient water. Hence, freshening of the HSSW both directly freshened and indirectly warmed the RSBW by enhancing the vertical mixing. A simple box model suggest that changes in property and volume transport (decrease of 6.7 % is assumed between the year 1995 and 2005) of the RSBW can explain 51 ± 6 % of the warming and 84 ± 10 % of the freshening observed in the AABW. These facts demonstrate that changes in both property and volume transport of the RSBW have contributed to the warming and freshening of the AABW in the Australian-Antarctic Basin.

OSD

8, 2197–2235, 2011

1 Introduction

Abyssal layer of the world ocean is supplied by the Antarctic Bottom Water (AABW) which originates from cold dense water formed by the formation of large volumes of sea ice in the Antarctic coastal polynyas. Thermohaline circulation, or overturning circulation, which is driven by the formation of dense water, makes an important contribution to the transport and storage of heat, carbon and other properties that influence climate. Understanding of formation process of the AABW, and its sensitivity to change, is therefore needed to improve projection of future climate change. The AABW which occupies abyssal layers of the Australian-Antarctic Basin is supplied by dense waters exported from the Ross Sea (Ross Sea Bottom Water, RSBW) and from the Adélie and George V Land (AGVL) region (Adélie Land Bottom Water, ALBW) (Rintoul, 1998; Williams et al., 2008, 2010). (As the focus of this paper is on the abyssal waters of the Australian-Antarctic Basin, we use AABW here to refer to this particular variety of bottom water.) The dense shelf waters formed by heat loss and addition of brine during sea ice formation in coastal polynyas entrain the relatively warm Circumpolar Deep Water (CDW) as they descend the continental slope. Both polynyas in the AGVL region and Ross Sea are regions of intense sea ice formation (Tamura et al., 2008) and hence dense water production. The inflows of the ALBW and the RSBW make the Australian-Antarctic Basin one of the best-ventilated basin in the Southern Ocean, based on the concentration of chlorofluorocarbons (CFCs) (Orsi et al., 1999).

The nature and causes of changes in properties of the AABW in the Australian-Antarctic Basin have been clarified in several recent studies. Whitworth (2002) concluded that two distinct modes of the AABW had been produced in the basin, with the cold, fresh mode more prevalent in later observations. Aoki et al. (2005), from comparison of CTD profiles from the same location and the season, reported evident freshening trend at 140° E from at least the early 1970s. Using the sections spanning the entire basin, Rintoul (2007) showed that freshening of the AABW was observed throughout the basin. The distribution of CFC-12 indicated that changes are limited

OSD
8, 2197–2235, 2011

to ventilated layer that had been in contact with the atmosphere within 55 yr (Johnson et al., 2008), consistent with the time scale of changes reported by Aoki et al. (2005) and Rintoul (2007). Changes in the abyssal waters of much of the world ocean have been traced back to the AABW, with the largest changes seen close to the Antarctic continent (Purkey and Johnson, 2010). In particular, changes in the AABW of the Australian-Antarctic Basin have been identified as the source of changes in the deep North Pacific (e.g., Kawano et al., 2009; Masuda et al., 2010). Identifying the process driving the changes in the AABW properties is therefore an important step in understanding changes in the overturning circulation.

Changes in the AABW could reflect changes in the properties, volume transport or mixing ratios of the sources of the dens waters to the Australian-Antarctic Basin. For example, the wide-spread freshening observed in recent decades could reflect an increased supply of melt water from ice shelves and glacier tongues. The rapid melt of floating ice in the Amundsen-Bellingshausen Seas has been identified as the likely source of the strong freshening trend observed in the shelf waters of the Ross Sea (Jacobs et al., 2002; Zwally et al., 2005; Jacobs and Giulivi, 2010). The changes in temperature of the AABW have more complicated distribution and are more difficult to explain. The AABW warmed over much of the basin between the years 1936–1993 and 1994–1996 (Whitworth, 2002), but cooled in the coastal region between 140 and 150° E from the year 1950 to 2001 (Jacobs, 2004, 2006) and at 140° E between the 1970s and 2002 (Aoki et al., 2005). These changes in temperature with space and time suggest that changes in the relative contribution of different source waters may have also played a role in observed changes in the AABW.

Several studies suggest that changes in the RSBW, and in its source waters the HSSW, are likely to contribute changes observed in the Australian-Antarctic Basin. Jacobs (2006) and Rintoul (2007) showed consistent freshening of the RSBW between the Ross Sea outflow and 150° E. Freshening of shelf waters in the Ross Sea have been attributed in part to inflow of glacial melt water from the east (Jacobs et al., 2002; Jacobs and Giulivi, 2010). Changes in sea ice formation likely also have played a role in

OSD
8, 2197–2235, 2011

recent freshening. Tamura et al. (2008) inferred a 30 % reduction in the volume of sea ice formed in the Ross Ice Shelf Polynya region from the end of the 1990s to the 2000s. Rivalo et al. (2010) reported that the export of dense water from the Western Ross Sea was 45 % lower in 2001 than in 1997. Therefore, change in both the properties and volume transport of the RSBW may have contributed to change in the AABW observed downstream.

In this study, we describe changes in the AABW properties based on CTD profiles of the WOCE Hydrographic Program (WHP) occupation in the 1990s and later repeat occupation in 2000s. Historical observations are used to track changes in the RSBW. A simple advective-diffusive model of the RSBW out flow is then developed to determine the contribution of changes in transport and mixing to the changes observed in the RSBW. Finally, influences of changes in property and volume transport of the RSBW on property of the AABW observe downstream are assessed.

2 Changes in property of the AABW in the Australian-Antarctic Basin

2.1 Changes in property of the AABW

A schematic illustrating the sources and circulation of the AABW in the Australian-Antarctic Basin is shown in Fig. 1. Dense waters formed in the AGVL region and the Ross Sea, after entraining the CDW as they descend the slope, supply the AABW, which flows westward over the continental slope and rise of Antarctica to the Kerguelen Plateau. The AABW turns north along the plateau until it joins the lower part of the Antarctic Circumpolar Current (ACC) to flow to the east (Orsi et al., 1999). The AABW exits the basin through the Princess Elisabeth Trough (PET) and through the Australian-Antarctic Discordance (AAD). The WHP sections (I8S, I9S, and SR3) cross the set of boundary currents transporting the AABW away from the source regions. Each of these sections was repeated in the 2000s (station locations are shown in Fig. 1 and details are given in Table 1). In this section, we describe changes in bottom water properties based on these data.

OSD
8, 2197–2235, 2011

The SR3 section crosses the AABW path just downstream of the inflow of the ALBW. Because this line is close to the source, near-bottom temperature and salinity vary with season and with location (e.g., Fukamachi et al., 2000). To minimize aliasing of seasonal and spatial variability, we focus on near-repeats of the same stations and in the same season. For the SR3, we supplement the October 2001 section with stations south of 61° S occupied in 2002 and 2003 in the same season as the original WHP line, to minimize seasonal aliasing (hereafter the combined profiles from 2001–2003 are simply referred to as 2001). The two repeats of the I9S were in the same season. At the I8S in the western side of the basin, the repeats were within 2 to 3 months of each other, and as the section is distant from the source regions we expect seasonal variability to be small. (No clear evidence of seasonal variability was observed in a two-year mooring array close to the I8S section, Fukamachi et al., 2010).

Changes in the AABW are illustrated by comparing the meridional variation of potential temperature, salinity, neutral density and apparent oxygen utilization (AOU) averaged over a 100 m-thick layer at the bottom for the WHP and repeat sections (Fig. 2). At the SR3, the potential temperature is lower in 2001 and 2008 than in the WHP south of 62° S. However, the lowest potential temperature (−0.72 °C) is in 2001 and the potential temperature in 2008 (−0.64 °C) is comparable to that of the WHP. Such a non-monotonic change suggests interannual variability in potential temperature. Cooling is also observed near 63° S at the I9S (−0.06 °C). However, warming is found further downstream along the entire I8S section and north of 61° S along the I9S (by up to 0.1 °C). The reversal of sign in the potential temperature changes is also observed in AOU: cooling is associated with a decrease in AOU on the I9S south of 62° S, and warming is associated with an increase in AOU at the I8S and north of 62° S on the I9S (Fig. 2b). While the changes in salinity do not reverse in sign, the freshening trend is intensified closer to the source regions (near the SR3 and at higher latitudes). In addition, the bottom layer is fresher in 2001 than in 2008 at SR3 (the minimum salinity south of 62° S is lower by 0.01). Hence, salinity also varies interannually. Near the sources of dense water (south of 62° S on the SR3 and near 63° S on the I9S), there

OSD
8, 2197–2235, 2011

is no clear change of density because cooling and freshening compensate each other. Further downstream (at the I8S and north of 61° S on the I9S), freshening and warming produce a decrease in density ($\sim 0.02\,\mathrm{kg\,m^{-3}}$).

Changes in the potential temperature-salinity diagram are illustrated in Fig. 3, following Johnson et al. (2008). Cooling and freshening on isopycnals is evident for water denser than $\gamma^n = 28.30$, indicating basin-wide changes in the AABW. Cooling and freshening on isopycnals reflects warming and/or freshening of water masses where the stratification is such that warmer, more saline waters overly cooler, fresher waters (i.e., density ratio > 1, Bindoff and McDougall, 1994). Thus, the changes in the AABW properties likely indicate warming or freshening of the sources of dense water.

Potential temperature and salinity differences on pressure surfaces are shown in Figs. 4 and 5. At the SR3, the strongest cooling is observed at the sea floor between 63° S and 64° S (Fig. 4d, e). At the I9S, warming dominates below $\gamma^n = 28.30$, although weak cooling is detected over the slope south of 62° S (Fig. 4c). Freshening dominates everywhere below $\gamma^n = 28.30$, with the strongest freshening at the sea floor (Fig. 5c). At the I8S, warming (Fig. 4a, b) and moderate freshening (Fig. 5a, b) are observed below $\gamma^n = 28.30$.

In summary, warming increases downstream and the freshening increases upstream along the pathway of the AABW. To obtain a rough estimate of the heat and freshwater fluxes needed to explain the observed patterns of change, we interpolated the changes observed at each section to the entire basin, using a Gaussian weighting function with an e-folding scale of 300 km and an influence radius of 1000 km. The overall warming of the AABW requires an input of $1300 \pm 200\,\mathrm{TW}$ of heat (or $0.37 \pm 0.05\,\mathrm{W\,m^{-2}}$) and $24\,\mathrm{Gt\,yr^{-1}}$ of freshwater (Table 2).

2.2 Possible causes of the observed changes

One possible cause of the observed freshening is a decrease in salinity of the dense shelf waters, as observed in the Ross Sea ($-0.03\,\mathrm{decade^{-1}}$ since the 1960s, Jacobs and Giulivi, 2010). No equivalent time series exists to assess changes in the salinity of

OSD
8, 2197–2235, 2011

dense shelf waters formed in the AGVL region. On the other hand, it is not straightforward to explain the warming of the AABW. The warming of the HSSW in the Ross Sea is trivial (2×10^{-3} °C decade^{-1}) and of the size expected from the change in freezing point temperature induced by the rapid freshening (Jacobs and Giulivi, 2010). Warming of the dense source waters therefore cannot explain the warming of the AABW. Other possible causes of warming include geothermal heat flux, horizontal or vertical diffusion, and reduced supply of cold dense shelf waters.

Among these candidates, the average geothermal heat flux for depths of 3500 to 4500 m is roughly 0.05–0.1 W m^{-2} (Stein and Stein, 1992). Even a 50 % increase would explain less than 15 % of the warming of the AABW and there is no reason to expect the geothermal heat flux to increase rapidly on decadal time-scales.

Horizontal diffusion is expected to carry a heat flux of about 0.01 W m^{-2}, using a basin-averaged horizontal temperature gradient at the depth of the $\gamma^n = 28.30$ isopycnal (8.9×10^{-7} °C m^{-1}) and a horizontal diffusivity of 2 m^2 s^{-1} (e.g., Ledwell, 1999). Hence horizontal diffusion cannot explain the observed warming. Polzin and Firing (1997) estimated a vertical diffusivity at 55° S on the I8S averaged below 1000 m of 4.4×10^{-4} m^2 s^{-1}. The basin-averaged vertical gradient of potential temperature at the depth of the $\gamma^n = 28.30$ isopycnal is 3.8×10^{-4} °C m^{-1}, implying a vertical diffusive heat flux of 0.67 W m^{-2}. Changes in the basin-averaged density stratification, which can affect both horizontal and vertical diffusion, were less than 10 % during the observational period. An increase in vertical diffusion of 10 % would explain only 19 % of the warming over the entire AABW layer. Hence, none of these processes can account for sufficient change in heat flux to explain the observed warming.

The spatial distribution of the observed changes is also an important factor. While the AABW warmed over most of the basin, cooling was observed near the source region. The fact that localized cooling is accompanied by a decrease in AOU and by significant freshening suggests a larger input of the cold, fresh source from the AGVL region relative to the input of relatively warm and salty inflow from the Ross Sea.

OSD
8, 2197–2235, 2011

The rough order of magnitude estimates of the contribution of various heat sources and the spatial distribution of changes in temperature and salinity support the hypothesis that a reduction in the inflow of the RSBW may have contributed to the changes observed in the basin. To examine this possibility in more detail, we consider an advective-diffusive balance for the waters between the Western Ross Sea and 150° E.

3 Changes in water masses property and advection-diffusion processes of the RSBW, and its impact on the AABW

3.1 Changes in property of the RSBW

Summer (January to March) hydrographic profiles along the approximate flow path of the RSBW in the region between the Drygalski Trough of the Western Ross Sea and 150° E were collected from World Ocean Database 2009 (Boyer et al., 2009). A total of 256 profiles reach within 50 m of the bottom, spanning the period from 1969 to 2004. Property changes of the RSBW are shown in Fig. 6. The RSBW freshened consistently from the 1970s and the bottom-intensified salinity maximum is drastically attenuated in the 2000s throughout the study area around 150° E (Fig. 6a), 160° E (Fig.6b), and in the vicinity of the source region (Fig. 6c). Warming is observed except near the source region. At 160° E, AOU averaged over the 100 m-thick layer at the bottom slightly increased in the 2000s (118.1 μmol kg^{-1}) compared to that in 1970s (114.1 μmol kg^{-1}; not shown).

Freshening of the RSBW can be explained by freshening of the HSSW, but warming of the RSBW cannot be explained by the observed warming of the HSSW (2×10^{-3} °C decade^{-1}). Since decreases in volume transport of the HSSW and hence the RSBW reduces the supply of both negative heat flux and oxygen rich water throughout its flow path, they are consistent with the property changes between the Drygalski Trough and 150° E. In the next subsection, we quantitatively estimate the change in volume transport of the RSBW by using a simple advection-diffusion model.

OSD
8, 2197–2235, 2011

3.2 A model of advection-diffusion process of the RSBW

The cold and saline HSSW flows out from the Drygalski Trough of the Western Ross Sea. The outflow sinks down the slope, entraining the ambient warm and relatively fresh (compared to the HSSW) CDW to form the RSBW. The RSBW is advected westward to 150° E with further warming and freshening induced by mixing with the ambient water. Hereafter, the dense water originating from the HSSW and sinking down the slope is referred to as the Modified Shelf Water (MSW) following Orsi and Wiederwohl (2009). Based on observations in the 1970s and 2000s, we will estimate the change in volume transport of the RSBW by analyzing changes in its advection-diffusion processes.

The governing diffusion equation of potential temperature of the RSBW can be written as follows.

$$\theta_t + u\theta_x + v\theta_y + w\theta_z = \frac{\partial}{\partial x}Kh\theta_x + \frac{\partial}{\partial y}Kh\theta_y + \frac{\partial}{\partial z}Kz\theta_z,$$

where x is flow path coordinate (downstream positive), y is the direction orthogonal to the flow path, and z is vertical axis (upward positive). Kz and Kh are vertical and horizontal diffusivities, respectively, and subscripts indicate the first order derivatives.

Starting from this general formula, we will simplify this equation based on the settings and approximations applicable in this case. As shown in Fig. 7, flow paths of the RSBW are bounded by the continental slope and sea floor in the direction of y and z, respectively, and fluxes through the two boundaries are zero. Hence, horizontal diffusion term of y axis and vertical diffusion terms are replaced by fluxes from the other side divided by the width Lo and thickness H of the RSBW, respectively.

$$\theta_t + u\theta_x + v\theta_y + w\theta_z = \frac{\partial}{\partial x}Kh\theta_x + \frac{1}{Lo}Kh\theta_y + \frac{1}{H}Kz\theta_z. \quad (1)$$

The third and fourth terms in the left hand side can be neglected since velocity orthogonal to the flow path and vertical velocity are negligible. The first term on the right

OSD
8, 2197–2235, 2011

hand side can be neglected because the horizontal gradient in the x-direction is negligible compared to gradients in the y and z directions. Equation (1) can therefore be simplified to:

$$\theta_t + u\theta_x = \frac{1}{Lo} Kh\theta_y + \frac{1}{H} Kz\theta_z . \quad (2)$$

Here, we will consider relative importance between the first and second terms in the right hand side. From Fig. 7, width Lo and thickness H of the RSBW can be estimated as 200 km and 200 m respectively and horizontal and vertical gradients were estimated as $\theta_y \approx 2.6 \times 10^{-6}\,^{\circ}\mathrm{C\,m^{-1}}$ and $\theta_z \approx 7.0 \times 10^{-4}\,^{\circ}\mathrm{C\,m^{-1}}$, respectively. No information on vertical diffusivity in the study area is available (Muench et al. (2009) estimated it in the vicinity of the source region but not for the remaining area. We will discuss this point later). However, Kunze et al. (2006) estimated average vertical diffusivity in the Southern Ocean by using strain profiles from CTD profiles and vertical velocity shear from LADCP. From Fig. 16 of Kunze et al. (2006), vertical diffusivity of near bottom can be the orders of 10^{-5}–$10^{-4}\,\mathrm{m^2\,s^{-1}}$. By adopting Osborn's (1980) model, vertical diffusivity Kz can be written in the following form of

$$Kz = 0.2\frac{\epsilon}{N^2} \quad (3)$$

where 0.2 is mixing efficiency, ϵ is energy dissipation rate, and N is Brunt–Väisälä frequency. ϵ is expected to be constant in time scale of our interest since dynamical background that drives turbulence remains unchanged. N^2 can be calculated from vertical profiles of observed data in following form of

$$N^2 = g(\beta S_z - \alpha\theta_z); \quad g = -9.8\ \mathrm{m\ s^{-2}} \quad (4)$$

Though absolute value of Kz is unknown due to the lack in observation of ϵ, rate of temporal change of Kz can be estimated by calculating N^2 for each period. Here, by using vertical diffusivity of Kunze et al. (2006), vertical flux takes value of 3.5×10^{-11} to $3.5 \times 10^{-10}\,^{\circ}\mathrm{C\,s^{-1}}$. By using $Kh = 2\,\mathrm{m^2\,s^{-1}}$ (e.g., Ledwell, 1999), horizontal fluxes

OSD
8, 2197–2235, 2011

takes value of 2.6×10^{-11} °C s^{-1}. Hence, the vertical diffusion term is likely one order larger than horizontal diffusion term. Even if the vertical diffusion does not dominate the horizontal diffusion, both vertical and horizontal diffusion are expected to act on the property of the RSBW in the same sense since the RSBW similarly mixes with the water of the CDW origin for both vertical and horizontal diffusion. Thus, by neglecting horizontal diffusion term, we obtain formula as

$$\theta_t + u\theta_x = \frac{1}{H} K_z \theta_z .$$

Now we will consider the uniform current ($u > 0$) throughout the flow path of the RSBW. There is no direct observation of u, but Fukamachi et al. (2000) measured current speed of 14.1 to 19.8 cm s^{-1} at slightly downstream (140° E). Pure downstream current speed could be somewhat smaller than the above value since current direction was not observed because the mooring was too close to the magnetic pole. But, if we assume the above value for downstream current speed, the time scale that advection carries the signal throughout the flow path of the 1000 km is 58 to 82 days. Hence, on the time scale we consider, temperature of this system will swiftly adjusted to the temperature induced at $x = 0$. Hence, for the case of multi-decadal variability, we obtain a formula as

$$\frac{\theta_z}{\theta_x} = \frac{uH}{K_z} \tag{5}$$

for each period of interest.

Equation (5) implies that the ratio of vertical gradient to horizontal gradient is determined by ratio of volume transport to vertical diffusivity. Horizontal velocity u determines residence time in the study area and, thus, determines the time scale which the RSBW is affected by vertical diffusion. Thickness H determines response of potential temperature of the RSBW against vertical diffusion. Both u and H proportionally contribute to maintain water mass property of the RSBW against the vertical diffusion. Hence, when volume transport uH takes large (small) value, horizontal gradient θ_x

OSD
8, 2197–2235, 2011

should takes small (large) value, and inversely, vertical gradient θ_z take large (small) value. On the other hand, vertical diffusivity Kz proportionally enhance vertical diffusion and thus, contribute to θ_x and θ_z in opposite sense against uH. Given the Eq. (5), we can estimate the temporal change in uH with estimating θ_x, θ_z, and N^2 based on the observed hydrographic profiles between the different periods whose interval is long enough.

Diffusion equation for salinity is also given in the same manner. Then, Eq. (5) is expressed as

$$uH = Kz\frac{\theta_z}{\theta_x} = Kz\frac{S_z}{S_x} \tag{6}$$

By substituting Eq. (3) into Eq. (6), we have the following equation.

$$uH^* = \frac{1}{N^2}\frac{\theta_z}{\theta_x} = \frac{1}{N^2}\frac{S_z}{S_x} \tag{7}$$

where $uH^* = uH/0.2\epsilon$. In the next subsection, we discuss change of volume transport by estimating Eq. (7) for respective period.

3.3 Change in advection-diffusion process of the RSBW

We analyzed data in the area from the Drygalski Trough to 900 km downstream (160° E), where most of the profiles are located along the flow path both in the 1970s and 2000s. As for the observations from 1985 to 1995, many of stations are deviated away from flow path and it is difficult to estimate the along-path process. Thus, Eq. (7) is evaluated for the 1970s and 2000s.

In the vicinity of the RSBW source region, waters which are not influenced by the HSSW are often found, reflecting the intermittent and narrow nature of the MSW plume. To exclude such profiles, OMP (Optimum Multiparameter) analysis is used to calculate the relative contributions of the HSSW and the Lower Circumpolar Deep Water (LCDW). The definition of each water type is shown in the appendix. Distribution of the

OSD
8, 2197–2235, 2011

HSSW fraction in the layer within 100 m of the bottom is shown in Fig. 8. In both the 1970s and 2000s, most of the profiles in upstream region within 150 km of the Drygalski Trough showed high HSSW fractions (> 0.4). In the downstream region beyond 150 km, on the other hand, the HSSW fraction is less than 0.2. This rapid decrease in fraction of the HSSW suggests that the MSW is governed by intensive mixing process including entrainment within the upstream region, and the RSBW properties become stable around 150 km downstream. Thus, we take the upstream region less than 150 km from the Drygalski Trough as the region of the modification of the MSW, and the downstream region beyond 150 km as the flow path of the RSBW. Along the flow path of the MSW, profiles showing extremely low fraction of the HSSW are most frequently found in the 2000s (Fig. 8). Hence, we analyze the flow path of the RSBW where profiles with extremely low fraction of the HSSW are not present and spatial density of the profiles is equivalent between the 1970s and 2000s.

In practice, the relative contribution of the large-scale pattern and small-scale variability along the flow path of the RSBW is different for temperature and salinity. While the large-scale pattern of temperature and its gradient are subject to significant small-scale perturbations, those of salinity and its gradient are dominant over small-scale spatial variations. Hence, we further conduct analysis based on salinity averaged over the 100 m-thick layer at the bottom and vertical gradients.

Distributions of salinity and its vertical gradient are shown in Fig. 9. To make all the areas are uniformly weighted, horizontal gradients are estimated by least square fit from the data averaged in 50 km interval bins for the two periods. Horizontal gradients of salinity in the 1970s and 2000s are estimated as $-3.86 \pm 0.59 \times 10^{-8}\,\mathrm{m}^{-1}$ and $-2.90 \pm 0.62 \times 10^{-8}\,\mathrm{m}^{-1}$, respectively (Table 3). Thus, with overall salinity declined throughout flow path of the RSBW, decrease in horizontal gradient from the 1970s to 2000s is estimated as approximately 25 %. Vertical gradients in 1970s and 2000s are estimated by taking means of bin averages (means of large circles in lower panels of Fig. 9) as $-8.94 \pm 0.71 \times 10^{-5}\,\mathrm{m}^{-1}$ and $-3.71 \pm 0.24 \times 10^{-5}\,\mathrm{m}^{-1}$, respectively. Decrease in vertical gradient by far exceeds that of horizontal gradient and estimated

OSD
8, 2197–2235, 2011

as approximately 59 %. Accordingly, ratios of vertical gradient and horizontal gradient in 1970s and 2000s are estimated as 2300 ± 400 and 1300 ± 300, respectively, and exhibits decrease of approximately 45 %. From Eq. (4), N^2 in 1970s and 2000s are $1.91 \pm 0.17 \times 10^{-6}\,s^{-2}$ and $1.34 \pm 0.05 \times 10^{-6}\,s^{-2}$, respectively, and decrease from the 1970s to 2000s is estimated approximately as 30 %. Substituting these estimates for Eq. (7), uH^* in the 1970s and 2000s are estimated as $12.1 \pm 2.3 \times 10^8\,s^2$ and $9.5 \pm 2.2 \times 10^8\,s^2$, respectively. Hence, the decrease in uH^* from 1970s to 2000s is estimated as 21 ± 23 %. Although the statistical significance is marginal, this result suggests decrease in volume transport of the RSBW.

These results suggest a reduction in the volume transport of the RSBW, associated with enhanced vertical diffusion as a result of weakening of the stratification (the decrease in N^2 is sufficient to increase the vertical diffusivity by 42 %). A reduction in volume transport is also consistent with the observed warming and increase in AOU of the RSBW.

3.4 Impact of changes in property and volume transport of the RSBW on characteristics of the AABW

The property changes of the RSBW are evident from the observation and a decrease in its volume transport of the RSBW is suggested as above. In this subsection, influence of property change and decrease in volume transport of the RSBW on the AABW is examined by a simple box model under some realistic assumptions.

Change in potential temperature of the AABW by supply of the RSBW for unit time can be represented as

$$-\frac{1}{V} V_{\mathrm{tr}} \Delta\theta, \tag{8}$$

where V_{tr} is volume transport of the RSBW supplied to the Australian-Antarctic Basin, $\Delta\theta$ is difference in potential temperature between the RSBW and the AABW, and V is total volume of the AABW. Here, V_{tr} and $\Delta\theta$ are expressed as sum of steady state

OSD
8, 2197–2235, 2011

component and fluctuation which is assume to increase in proportion to time, i.e., $V_{tr} = \overline{V_{tr}} + \delta V_{tr} t$ and $\Delta\theta = \overline{\Delta\theta} + \delta\Delta\theta t$. Substitution of these into Eq. (8) gives,

$$-\frac{1}{V}\left(\overline{V_{tr}}\,\overline{\Delta\theta} + \overline{V_{tr}}\delta\theta t + \overline{\Delta\theta}\delta V_{tr} t + \delta\theta\delta V_{tr} t^2\right) \tag{9}$$

The first term in the bracket is steady state component which is assumed to be balanced with steady state heat flux in the basin due to vertical and horizontal diffusion and geothermal heat. Here we are interested in the fluctuation components which deviate from the balance, and thus, we neglect the first term and the fourth infinitesimal term. By integrating the above equation with respect to time, warming of the AABW due to the RSBW influence ($\Delta\theta_{RSBW}$) by temporal changes in property and volume transport of the RSBW can be considered. Corresponding freshening of the AABW due to the RSBW influence (ΔS_{RSBW}) is also given by the same procedure. For the integrating time T, we will have

$$\Delta\theta_{RSBW} = -\frac{1}{V}\left(\overline{V_{tr}}\delta\theta + \overline{\Delta\theta}\delta V_{tr}\right)\frac{T^2}{2}$$
$$\Delta S_{RSBW} = -\frac{1}{V}\left(\overline{V_{tr}}\delta S + \overline{\Delta S}\delta V_{tr}\right)\frac{T^2}{2} \tag{10}$$

The first term in the right hand side of Eq. (10) is the component due to the changes in property of the RSBW and the second term is the component due to the decrease in volume transport.

Contributions of temperature and salinity changes from the RSBW are then estimated using Eq. (10) for the period of 10 yr from 1995 to 2005, following the observational period in the Australian-Antarctic Basin. The trend in potential temperature and salinity of the RSBW is evaluated by the regression line for bottom water property averaged over 100 m-thick layer at bottom around 150° E (Fig. 10).

Potential temperature and salinity of the AABW in the year 1995 and 2005 are calculated by basin average estimated by using all the data shown in Table 1 and the trends

OSD
8, 2197–2235, 2011

shown in Table 2a, respectively. Above average are estimated by the same interpolation procedure as that in the Sect. 2.1. Then, $\delta\theta$ and δS are estimated by changing rate of difference between the RSBW and the AABW as

$$\delta\theta = \frac{\Delta\theta_{2005} - \Delta\theta_{1995}}{T}, \quad \delta S = \frac{\Delta S_{2005} - \Delta S_{1995}}{T}.$$

Steady state component of volume transport $\overline{V_{\mathrm{tr}}}$ of the RSBW is required in this formulation. Temporal and spatial mean potential temperature (−0.36 °C) and salinity (34.70) around 150° E (Fig. 10) gives approximate mixing ratio of the HSSW and the LCDW as 1 : 6. This implies that the HSSW exported from the Drygalski Trough entrained the LCDW whose volume is 6 times larger than the HSSW during advection. Then, adopting the export value of the HSSW from the Drygalski Trough (0.98 Sv) estimated by Whitworth and Orsi (2006), $\overline{V_{\mathrm{tr}}}$ at 150° E is assumed to be 7 Sv.

With the above $\overline{V_{\mathrm{tr}}}$ and observed $\delta\theta$ and δS, the change in property of the RSBW can explain 44 ± 5 % and 63 ± 8 % of overall warming and freshening of the AABW. The change rate in volume transport δV_{tr} is the largest unknown in Eq. (10). Hence, we consider possible two scenarios. For the scenario 1, we assume that the decrease of volume transport of the RSBW from 1995 to 2005 is 6.7 %. This value is based on suggested decrease in volume transport of the RSBW (≈ 20 %/30 yr) derived in the Sect. 3.2. For the scenario 2, we assume that the decrease of volume transport of 20 %, which reflects the rapid decrease in sea ice production pointed out by Tamura et al. (2008).

Hereafter we evaluate $\Delta\theta_{\mathrm{RSBW}}$ and ΔS_{RSBW} using Eq. (10) according to two scenarios for decrease in volume transport (Table 4). For the scenario 1, $\Delta\theta_{\mathrm{RSBW}}$ can explain 51 ± 6 % of the overall warming of the AABW. Contribution of the change in property (first term) by far exceeds that of the change in volume transport (second term). ΔS_{RSBW} can explain 84 ± 10 % of the overall freshening of the AABW and similarly as in the case of the $\Delta\theta_{\mathrm{RSBW}}$, contribution of the first term by far exceeds that of the second term. For the scenario 2, the second term largely increased and $\Delta\theta_{\mathrm{RSBW}}$

OSD
8, 2197–2235, 2011

and ΔS_{RSBW} take value 63 ± 8 % and 131 ± 16 % of the overall warming and freshening of the AABW, respectively. In this case, the second term is comparable to the first term as for freshening, while it is approximately only a half of the first term as for warming.

Hence, the change in properties of the RSBW can explain nearly a half of the observed change of the AABW, and the decrease in volume transport of the RSBW can also be significant especially with the larger decrease with time.

4 Discussion

Property changes observed in the AABW require a heat and freshwater input of 1300 TW and 24 Gt yr^{-1}, respectively (the Sect. 2). The inferred rate of warming (0.37 ± 0.05 W m^{-2}) of the AABW that supplies the abyssal basin deeper than 3000 m is comparable to that of the world ocean warming (0.20 W m^{-2}) between 1955 and 1998 (Levitus et al., 2005), a large part of which occurs above 700 m depth. The observed freshening is about half of the freshening rate on the shelf and over the gyre reported by Jacobs et al. (2002). Errors are estimated from the multiple occupations of SR3, as only one repeat of the other sections is available.

Changes in the RSBW are inferred to be one of the major factors driving the changes observed in the AABW (the Sect. 3). Both enhanced vertical diffusion as a result of weakening stratification and a decrease in volume transport of the RSBW are likely to contribute to the warming and increase in AOU of the RSBW, and to the changes in AABW observed downstream. However, this conclusion rests on numerous assumptions. Here we discuss the robustness and consistency of the results.

Horizontal diffusion was assumed to be small (Eq. 2). The validity of this approach can be tested by confirming consistency between the observed vertical diffusivity (Muench et al., 2009) and that we adopted in this study. Based on Eq. (6), Kz can be expressed as:

$$Kz = \frac{uH}{\theta_z/\theta_x} = \frac{uH}{S_z/S_x}$$

OSD
8, 2197–2235, 2011

uH can be estimated as $19.6\,m^2\,s^{-1}$ from export of the HSSW from the Drygalski Trough of 0.98 Sv (Whitworth and Orsi, 2006) and width of the Drygalski Trough as 50 km. By using S_z/S_x in the 1970s (2314) and 2000s (1278), adopted Kz can be estimated as $0.84\times10^{-2}\,m^2\,s^{-1}$ and $1.53\times10^{-2}\,m^2\,s^{-1}$, respectively. These values are consistent with the order (10^{-2}–$10^{-3}\,m^2\,s^{-1}$) observed in the vicinity of the Drygalski Trough by Muench et al. (2009). This consistency suggests that observed changes in property along the flow path can be explained by vertical flux alone and does not require other flux sources. Hence, it is expected that the fact that we neglected horizontal diffusion would not be a fatal issue. However, due to lack in direct observation of both vertical diffusivity and volume transport in further downstream, it is difficult to fully examine this problem.

In estimating the influence of changes in the RSBW on the AABW, we assumed a box model of Eq. (10) in the Sect. 3.3. As for the volume transport of the RSBW V_{tr}, we used 7 Sv by considering export of the HSSW from the Drygalski Trough (0.98 Sv) estimated by Whitworth and Orsi (2006) and subsequent entrainment of the LCDW based on bottom temperature-salinity relation around 150° E. This transport of 7 Sv corresponds to average westward velocity of $17.5\,cm\,s^{-1}$ over the area of width and thickness of the RSBW of 200 km and 200 m, respectively at 150° E, hence it is consistent with the velocity assumed in the advection-diffusion model in the Sect. 3.2 based on the mooring observations (Fukamachi et al., 2000). Validity of this value can also be examined by considering the steady state heat balance in the AABW. Heat flux induced by supply of the RSBW with volume transport of 7 Sv is estimated as $-0.71\,W\,m^{-2}$ and this can be balanced by the heat flux induced by vertical diffusion discussed in the Sect. 2.2 ($0.67\,W\,m^{-2}$). Although there are some limitations such as scarce information of the influence by supply of the dense shelf water in the AGVL region, uncertainty of effect of horizontal diffusion, uncertainty of the vertical diffusivity estimated by Polzin and Firing (1997), it is expected that assumed volume transport would also be supported in the first order.

OSD
8, 2197–2235, 2011

While the decrease in volume transport of the RSBW can be explained by a decrease in the HSSW, how can the weakening of the density stratification be explained? Weakening of vertical gradients of potential temperature and salinity from the 1970s to 2000s are approximately 17 % and 59 %, respectively, and they account for 32 % and 68 % of the decrease in N^2, respectively. The decrease in the vertical gradient of salinity can, in turn, be explained by the long-term freshening of HSSW (Jacobs and Giulivi, 2010), which implies a reduction in the salinity contrast between RSBW and the relatively fresh ambient water. Hence, we suggest that freshening of the HSSW also warmed the RSBW by enhancing the vertical diffusion of heat by weakening the density gradient.

5 Summary and conclusions

The WHP and repeated hydrographic data were used to examine changes in the AABW in the Australian-Antarctic Basin. Changes in average potential temperature and salinity below $\gamma^n = 28.30$ suggest basin-wide warming (1300 ± 200 TW) and freshening (24 ± 3 Gt yr^{-1}) of the AABW. The RSBW also warmed, at a more rapid rate than its source waters. A 21 ± 23 % reduction in the volume transport of the RSBW and enhanced vertical diffusion of heat as a result of a 30 ± 7 % decrease in density stratification are inferred to drive the warming. Freshening of the HSSW enhanced vertical mixing by reducing the salinity stratification between RSBW and the overlying ambient water. Hence, we propose that the freshening of the HSSW directly freshened the RSBW downstream, and indirectly warmed the RSBW by enhancing vertical mixing. A simple box model suggests that changes in the properties and volume transport of RSBW can explain 51 ± 6 % of the warming of the AABW and 84 ± 10 % of the freshening.

Observations revealed the presence of significant interannual variability of the AABW in this basin. However, interannual variability at the I8S and the I9S could not be taken into account because only two occupations of these lines were available. In addition,

OSD
8, 2197–2235, 2011

trends in the properties of the RSBW, used in the evaluation of the influence of the RSBW changes on the AABW, are based on observations between the 1970s and 1990s since no data were available from after 1996 near 150° E.

Long-term changes in the dense shelf water formed in the AGVL region may also be important, but could not be estimated because of the lack of long-term observations in the area. Furthermore, it is pointed out from model study that the calving of the Mertz Glacier tongue in this region, which occurred on 12 to 13 February 2010, can reduce export of the Dense Shelf Water by 23 % with an unignorable decrease in density of exported water (Kusahara et al., 2010). Given that this type of event occur on decadal to centenary time-scales, influence on both the Dense Shelf Water and the AABW can be extensive. Hence, it is highly desirable to continue ongoing measurements programs in this area.

As the steady state volume transport of the RSBW is a key parameter that determines the influence of the RSBW change on the AABW, better observations of flow rates would help to clarify the cause of changes observed in the AABW. Further observations along the flow path from the Ross Sea to the Australian-Antarctic Basin are needed to monitor the change and estimate the impact on the AABW.

Appendix A

Application of the OMP analysis

In this study we used Optimum Multiparameter (OMP) analysis to discern profiles which are not influenced by the HSSW in vicinity of the slope by defining water type of the HSSW and the LCDW. The OMP analysis is introduced by Tomczak (1981), and Tomczak and Large (1989) to estimate spatial distribution of water masses and their mixing process. As for potential temperature of the LCDW, we adopt 0 °C for both periods of the 1970s and 2000s and corresponding salinity of 34.70 and 34.685 are given from θ–S diagram. As for potential temperature and salinity of the HSSW, those of each

OSD
8, 2197–2235, 2011

period are adopted from regression lines shown in Fig. 3 of Jacobs and Giulivi (2010), which presented long term trend of both potential temperature and salinity of the HSSW (as for the 1970s: $\theta = -1.89\,^{\circ}\mathrm{C}$, $S = 34.83$, as for the 2000s: $\theta = -1.87\,^{\circ}\mathrm{C}$, $S = 34.74$).

Acknowledgements. This work was supported by the fund from Grant-in-Aids for Scientific Research (20221001 and 21310002) of the Japanese Ministry of Education, Culture, Sports, Science and Technology.

References

Aoki, S., Rintoul, S. R., Ushio, S., Watanabe, S., and Bindoff, N. L.: Freshening of the Adélie Land Bottom Water near 140° E, Geophys. Res. Lett., 32, L23601, doi:10.1029/2005GL024246, 2005.

Bindoff, N. L. and Mcdougall, T. J.: Diagnosing climate change and ocean ventilation using hydrographic data, J. Phys. Oceanogr., 24, 1037–1152, 1994.

Boyer, T. P., Antonov, J. I., Baranova, O. K., Garcia, H. E., Johnson, D. R., Locarnini, R. A., Mishonov, A. V., O'Brien, T. D., Seidov, D., Smolyar, I. V., and Zweng, M. M.: World Ocean Database 2009, in: NOAA Atlas NESDIS 66, edited by: S. Levitus, US Gov. Printing Office, Wash., D.C., 216 pp., DVDs, 2009.

Fukamachi, Y., Wakatsuchi, M., Taira, K., Kitagawa, S., Ushio, S., Takahashi, A., Oikawa, K., Furukawa, T., Yoritaka, H., Fukuchi, M., and Yamanouchi, T.: Seasonal variability of bottom water properties off Adélie Land, Antarctica, J. Geophys. Res., 105, 6531–6540, 2000.

Fukamachi, Y., Rintoul, S. R., Church, J. A., Aoki, S., Sokolov, S., Rosenberg, M. A., and Wakatsuchi, M.: Strong export of Antarctic Bottom Water east of the Kerguelen plateau, Nat. Geosci., 3, 327–331, doi:10.1038/ngeo842, 2010.

Jacobs, S. S.: Bottom water production and its links with the thermohaline circulation, Antarct. Sci., 16, 427–437, 2004.

Jacobs, S. S.: Observations of change in the Southern Ocean, Philos. T. R. Soc. A., 364, 1657–1681, doi:10.1098/rsta.2006.1794, 2006.

Jacobs, S. S. and Giulivi, C. F.: Large multidecadal salinity trends near the Pacific-Antarctic Continental Margin, J. Climate, 23, 4508–4524, 2010.

Jacobs, S. S., Giulivi, C. F., and Mele, P. A.: Freshening of the Ross Sea during the late 20th century, Science, 297, 386–389, 2002.

OSD

8, 2197–2235, 2011

Jonson, G. C., Purkey, S. G., and Bullister, J. L.: Warming and freshening in the Abyssal Southeastern Indian Ocean, J. Climate, 21, 5351–5363, 2008.
Kawano, T., Doi, T., Uchida, H., Kouketsu, S., Fukasawa, M., Kawai, Y., and Katsumata, K.: Heat content change in the Pacific Ocean between the 1990s and 2000s, Deep Sea-Res. II, 57, 1141–1151, 2009.
Kunze, E., Firing, E., Hummon, J. M., Chereskin, T. K., and Thurnherr, A. M.: Global Abyssal Mixing Inferred from Lowered ADCP Shear and CTD Strain Profiles, J. Phys. Oceanogr., 36, 1553–1576, 2006.
Kusahara, K., Hasumi, H., Williams, G. D.: Impact of the Mertz Glacier Tongue calving on dense water formation and export, Nature Communications, 2, 159, doi:10.1038/ncomms1156, 2011
Ledwell, J. R., Watson, A. J., and Law, C. S.: Mixing of a tracer in the pycnocline, J. Geophys. Res., 103, 21499–21529, 1998.
Levitus, S., Antonov, J., and Boyer, T.: Warming of the world ocean, 1955–2003, Geophys. Res. Lett., 32, L23601, doi:10.1029/2004GL021592, 2005.
Masuda, S., Awaji, T., Sugiura, N., Mathews, J. P., Toyoda, T., Kawai, Y., Doi, T., Kouketsu, S., Igarashi, H., Katsumata, K., Uchida, H., Kawano, T., and Fukasawa, M.: Simulated rapid warming of Abyssal North Pacific Waters, Science., 329, 319–322, 2010.
Muench, R., Padman, L., Gordon, A., and Orsi, A.: A dense water outflow from the Ross Sea, Antarctica: mixing and the contribution of tides, J. Marine Syst., 77, 369–387, 2009.
Polzin, K. L. and Firing, E.: Estimates of diapycnal mixing using LADCP and CTD data from I8S, International WOCE Newsletter, 29, 39–42, 1997.
Orsi, A. H. and Wiederwohl, C. L.: A recount of Ross Sea waters, Deep-Sea Res. II, 56, 778–795, 2009.
Orsi, A. H., Johnson, G. C., and Bullister, J. L.: Circulation, mixing, and production of Antarctic Bottom Water, Prog. Oceanogr., 43, 55–109, 1999.
Osborn, T. R.: Estimates of the local rate of vertical diffusion from dissipation measurements, J. Phys. Oceanogr., 10, 83–89, 1980.
Purkey, S. G. and Johnson, G. C.: Warming of global Abyssal and deep Southern Ocean waters between the 1990s and 2000s: contribution to global heat and sea level rise budgets, J. Climate, 23, 6336–6351, 2010.
Rintoul, S. R.: On the origin and influence of Adélie Land Bottom Water, ocean, ice and atmosphere: interactions at Antarctic Continental Margin, Antarct. Res. Ser., 75, 151–171,

OSD
8, 2197–2235, 2011

1998.
Rintoul, S. R.: Rapid freshening of Antarctic Bottom Water formed in the Indian and Pacific Oceans, Geophys. Res. Lett., 34, L06606, doi:10.1029/2006GL028550, 2007.
Rivaro, P., Massolo, S., Bergamasco, A., Castagno, P., and Budillon, G.: Chemical evidence of the changes of the Antarctic Bottom Water ventilation in the Western Ross Sea between 1997 and 2003, Deep-Sea Res. I, 57, 639–652, 2010.
Stein, C. and Stein, S.: A model for the global variation in oceanic depth and heat flow with lithospheric age, Nature, 359, 123–129, 1992.
Tamura, T., Ohshima, K. I., and Nihashi, S.: Mapping of sea ice production for Antarctic coastal polynyas, Geophys. Res. Lett. 35, L07606, doi:10.1029/2007GL032903, 2008.
Tomczak, M.: A multiparameter extension of the temperature/salinity diagram techniques for the analysis of non-isopycnal mixing, Prog. Oceanogr. 10, 147–171, 1981.
Tomczak, M. and Large, D. G. B.: Optimum multiparameter analysis of mixing in the thermocline of the Eastern Indian Ocean, the temperature/salinity diagram techniques for the analysis of non-isopycnal mixing, J. Geophys. Res. 94, 16141–16149, 1989.
Whitworth, T.: Two modes of bottom water in the Australian-Antarctic Basin, Geophys. Res. Lett. 29, 1073, doi:10.1029/2001GL014282, 2002.
Whitworth, T. and Orsi, A. H.: Antarctic Bottom Water production and export by tides in the Ross Sea, Geophys. Res. Lett. 33, L12609, doi:10.1029/2006GL026357, 2006.
Williams, G. D., Bindoff, N. L., Marsland, S. J., and Rintoul, S. R.: Formation and export of dense shelf water from the Adélie Depression, East Antarctica, J. Geophys. Res., 113, C04039, doi:10.1029/2007JC004346, 2008.
Williams, G. D., Aoki, S., Jacobs, S. S., Rintoul, S. R., Tamura, T., and Bindoff, N. L.: Antarctic Bottom Water from the Adélie and George V Land coast, East Antarctica (140–149° E), J. Geophys. Res., 115, C04027, doi:10.1029/2009JC005812, 2010.
Zwally, H. J., Giovinetto, M. B., Li, J., Cornejo, H. G., Beckley, M. A., Brenner, A. C., Saba, J. L., and Yi, D. H.: Mass changes of the Greenland and Antarctic ice sheets and shelves and contribution to sea-level rise. 1992–2002, J. Glaciol., 51, 509–527, 2005.

OSD
8, 2197–2235, 2011

Table 1. Summary of the WOCE WHP and repeat occupations. The WOCE WHP section designation, years and months and latitudinal range of the WHP and repeat occupations, cruise code names, vessels used for repeat occupations and time intervals.

WOCE WHP Sections	WHP occupation months and year	WHP occupation latitudinal range	Repeat occupation months and year	Repeat occupation latitudinal range	Repeat occupation cruise-R/V	Time interval (year)
SR3	Jan–Feb 1995	50–66° S	Oct–Nov 2001/ Feb 2002, 2003	50–61° S/ 61–66° S	AU0103-RSV *Aurora Australis*/ JARE43, 44 *Tangaroa*	6/ 7, 8
			Mar–Apr 2008	50–66° S	AU0806-RSV *Aurora Australis*	13
I9S	Jan 1995	50–66° S	Jan 2005	50–66° S	AU0403-RSV *Aurora Australis*	10
I8S	Dec 1994/ Jan1995	47–64° S/ 64–66° S	Feb–Mar 2007	47–66° S	US Repeat Hydrography Program-R/V *Roger Revelle*	12

OSD
8, 2197–2235, 2011

Table 2a. Basin and section averaged trends in property of the AABW in the Australian-Antarctic Basin. Total volume of layers below isopycnal of $\gamma^n = 28.30$, mean potential temperature trend, required heat flux, mean salinity trend, required freshwater input in the Australian-Antarctic Basin.

	Australian-Antarctic Basin
Volume (km^3)	2.54×10^6
$\Delta\theta$ ($^\circ C\,decade^{-1}$)	$4.09 \pm 0.53 \times 10^{-2}$
Heat input	1322 ± 172 (TW)/0.37 ± 0.05 ($W\,m^{-2}$)
ΔS ($decade^{-1}$)	$-2.67 \pm 0.42 \times 10^{-3}$
Fresh water input ($Gt\,yr^{-1}$)	24.0 ± 3.2

OSD
8, 2197–2235, 2011

Table 2b. Basin and section averaged trends in property of the AABW in the Australian-Antarctic Basin. Section averaged thickness of layers below isopycnals of $\gamma^n = 28.30$, potential temperature trends, required heat fluxes, salinity trends, required freshwater inputs for respective sections. Error ranges for the SR3 were derived from 95 % confidence limit of linear regression coefficient.

	I8S (40–60° S)	I8S (60–67° S)	I9S	SR3
Thickness (m)	761	840	838	695
$\Delta\theta$ (°C decade^{-1})	7.65×10^{-2}	4.22×10^{-2}	3.72×10^{-2}	$2.14 \pm 2.41 \times 10^{-2}$
Heat flux (W m^{-2})	0.75	0.46	0.40	0.19 ± 0.22
ΔS (decade^{-1})	-1.15×10^{-3}	-2.82×10^{-3}	-3.14×10^{-3}	$-4.22 \pm 2.24 \times 10^{-3}$
Fresh water input (mm m^{-2} yr^{-1})	3.5	7.5	8.3	9.0 ± 4.6

OSD
8, 2197–2235, 2011

Table 3. Mean vertical salinity gradients, horizontal salinity gradients, their ratios, N^2 and uH^* for the RSBW in the 1970s and 2000s from region between 150 km and 900 km downstream from the Drygalski Trough.

	1970s	2000s
S_z (m^{-1})	$-8.94 \pm 0.71 \times 10^{-5}$	$-3.71 \pm 0.24 \times 10^{-5}$
S_x (m^{-1})	$-3.86 \pm 0.59 \times 10^{-8}$	$-2.90 \pm 0.62 \times 10^{-8}$
S_z/S_x	2300 ± 400	1300 ± 300
N^2 (s^{-2})	$1.91 \pm 0.17 \times 10^{-6}$	$1.34 \pm 0.05 \times 10^{-6}$
uH^* (s^2)	$12.1 \pm 2.3 \times 10^8$	$9.5 \pm 2.2 \times 10^8$

OSD
8, 2197–2235, 2011

Table 4. Possible warming and freshening of the AABW induced by change in property, decrease in volume transport of the RSBW, and their summations under the two scenarios of volume transport decrease of 6.7 %/10 yr and 20 %/10 yr. Results are shown in the form of ratio to the overall warming and freshening of the AABW estimated in the Sect. 2. Subscripts "1" denote contribution by change in property (first term in right hand side of Eq. 10) and subscript "2" denote contribution by decrease in volume transport of the RSBW (second term in right hand side of Eq. 10).

	Scenario 1 (6.7 %)	Scenario 2 (20 %)
$\Delta\theta_{\mathrm{RSBW\_1}}$	44 ± 5 %	44 ± 5 %
$\Delta\theta_{\mathrm{RSBW\_2}}$	6 ± 1 %	19 ± 2 %
$\Delta\theta_{\mathrm{RSBW}}$	51 ± 6 %	63 ± 8 %
$\Delta S_{\mathrm{RSBW\_1}}$	61 ± 8 %	61 ± 8 %
$\Delta S_{\mathrm{RSBW\_2}}$	23 ± 3 %	69 ± 9 %
ΔS_{RSBW}	84 ± 10 %	131 ± 16 %

OSD
8, 2197–2235, 2011

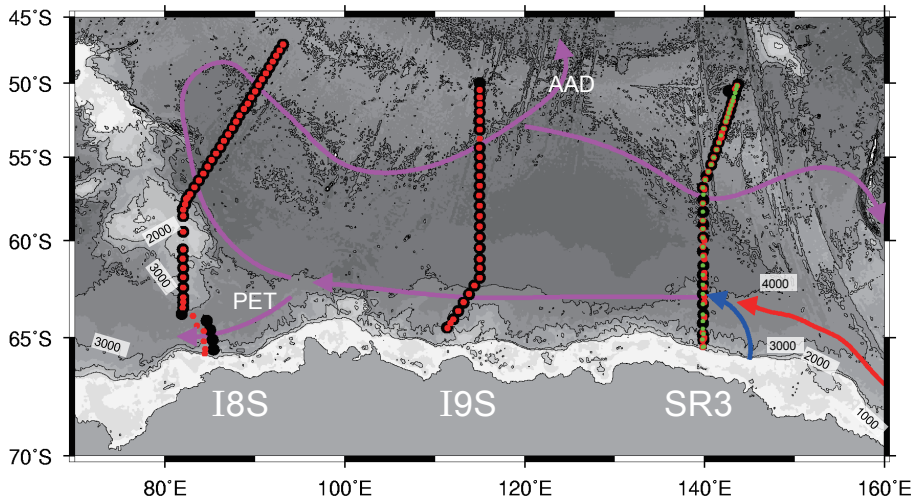

Fig. 1. Locations of the WOCE WHP (black circles) and their repeat (red and green circles) meridional hydrographic sections crossing the Australian-Antarctic Basin with schematic view of spreading path of the AABW. Red circles on the SR3 show locations of repeat occupations in the year 2001 (50–61° S), 2002 (61–66° S), 2003 (61–66° S) and green circles show those in 2008, respectively. All the red circles on both the I9S and I8S show repeat occupations in the 2000s. Red and blue arrows indicate the RSBW from the Ross Sea and ALBW from the AGVL region respectively and the AABW is indicated by purple arrows.

OSD
8, 2197–2235, 2011

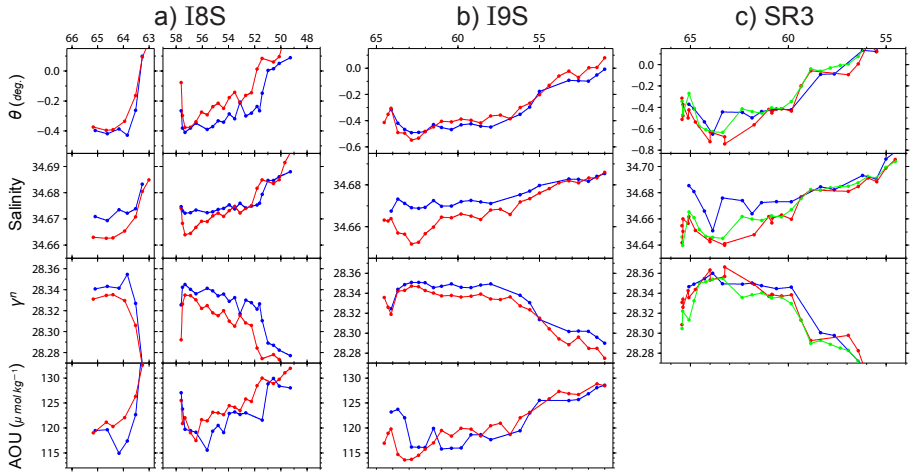

Fig. 2. Meridional variations of the water property averaged over the 100 m-thick layer at the bottom for **(a)** the I8S, **(b)** the I9S and **(c)** the SR3. Blue circles and lines are from the WHP occupations in the 1990s. Red circles and lines in **(c)** are from repeat occupations in the year 2001 (50–61° S), 2002 (61–66° S), 2003 (61–66° S) and green circles and lines in **(c)** are from those in 2008. All the red circles and lines in both **(a)** and **(b)** are from repeat occupations in the 2000s.

OSD
8, 2197–2235, 2011

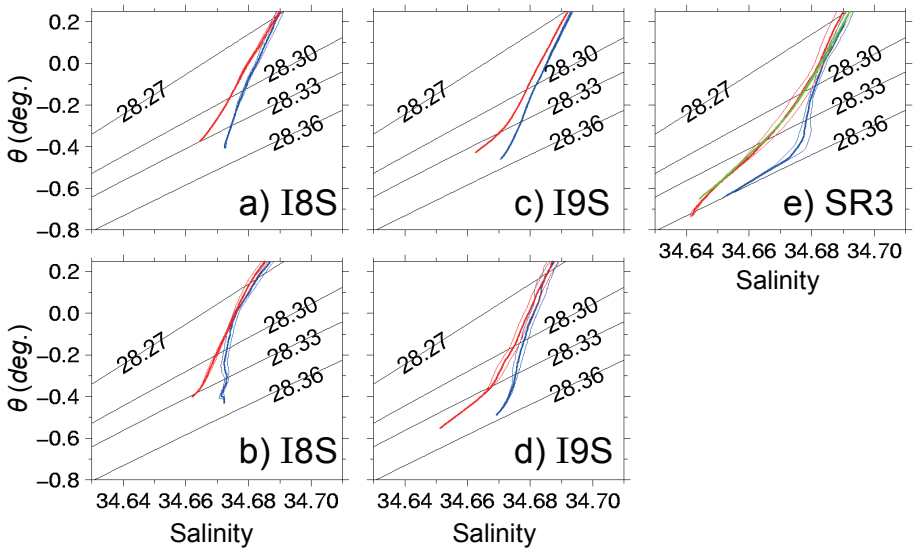

Fig. 3. Variations of $\theta - S$ curves for **(a)** the I8S (46–60° S, the Australian-Antarctic Basin), **(b)** the I8S (60–67° S, the PET), **(c)** the I9S (50–61° S), **(d)** the I9S (61–66° S) and **(e)** the SR3. Data are averaged on the isopycnal surfaces. Means are shown by thick lines and one standard deviation envelopes are shown by thin lines. Blue lines are from the WHP occupations in the 1990s. Red lines in e are from repeat occupations in the year 2001, 2002, 2003 and green lines in e are from in the year 2008. All the red lines in other panels are from repeat occupations in the 2000s. Labeled black lines are contour of neutral density.

OSD
8, 2197–2235, 2011

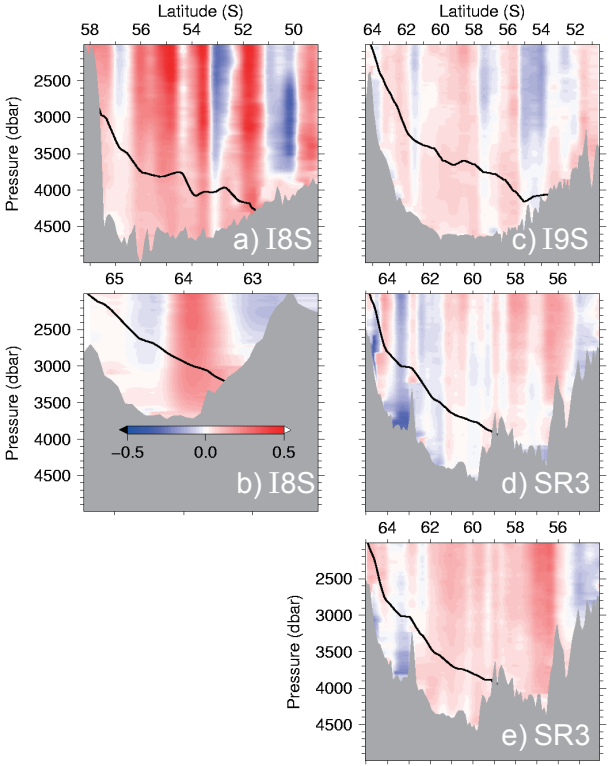

Fig. 4. Difference in isobaric potential temperature between the WHP and repeat occupations with the mean isopycnal of $\gamma^n = 28.30$. Red areas indicate warming and blue areas indicate cooling. **(a)** the I8S (the Australian-Antarctic Basin), **(b)** the I8S (the PET), **(c)** the I9S, **(d)** the SR3 (obtained from subtracting the WHP from combined repeat occupations in the year 2001, 2002, and 2003), **(e)** the SR3 (obtained from subtracting the WHP from repeat occupations in the year 2008). Mean isopycnals of $\gamma^n = 28.30$ are shown by solid lines.

OSD
8, 2197–2235, 2011

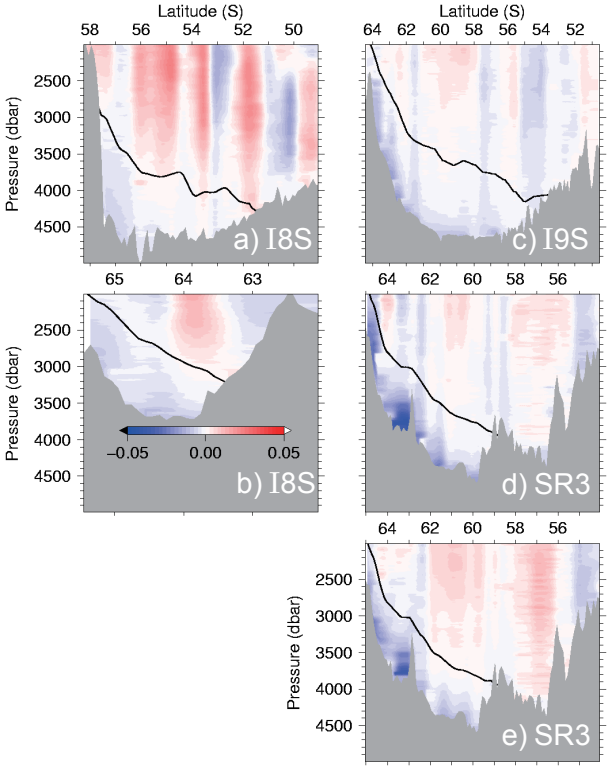

Fig. 5. Difference in isobaric salinity between the WHP and repeat occupations with the mean isopycnal of $\gamma^n = 28.30$. Red areas indicate increase in salinity and blue areas indicate freshening. **(a)** the I8S (the Australian-Antarctic Basin), **(b)** the I8S (the PET), **(c)** the I9S, **(d)** the SR3 (obtained from subtracting the WHP from combined repeat occupations in the year 2001, 2002, and 2003), **(e)** the SR3 (obtained from subtracting the WHP from repeat occupations in the year 2008). Mean isopycnals of $\gamma^n = 28.30$ are shown by solid lines.

OSD
8, 2197–2235, 2011

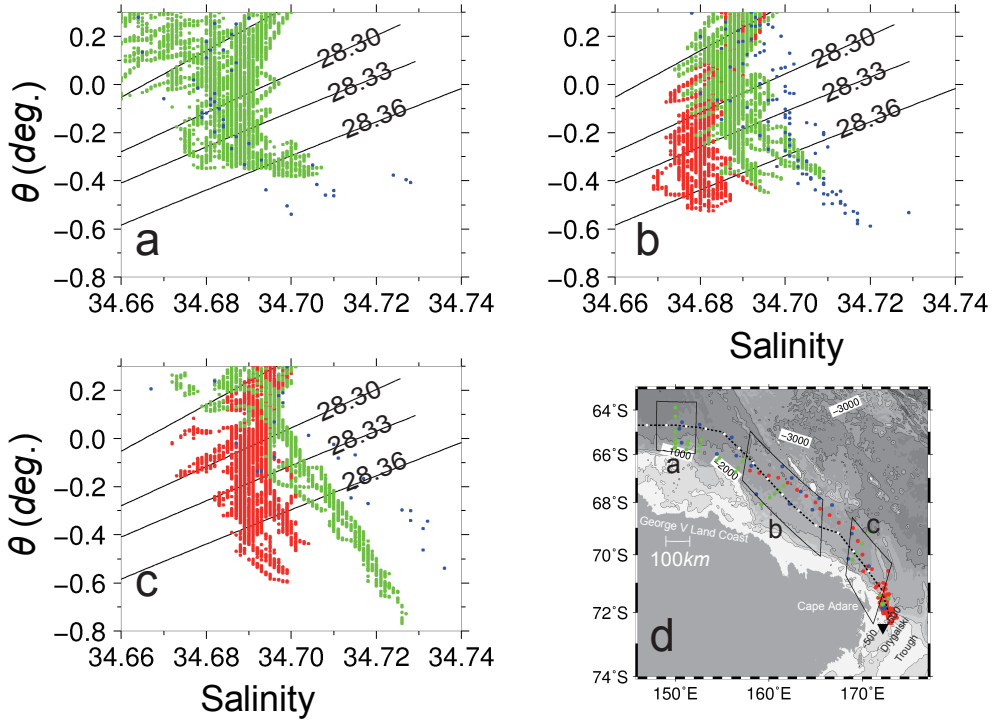

Fig. 6. *θ–S* diagrams of region between the Drygalski Trough and 150° E. **(a)** around 150° E, **(b)** around 160° E, **(c)** immediately downstream of the Ross source region, **(d)** locations of stations. Blue circles are from occupations in the 1970s, green circles are from 1990s and red circles are from 2000s. Labeled black lines in **(a)**, **(b)**, and **(c)** are contour of neutral density. Dashed line in d indicates approximate position of flow path of the RSBW and white circles are marked on 100 km interval.

OSD
8, 2197–2235, 2011

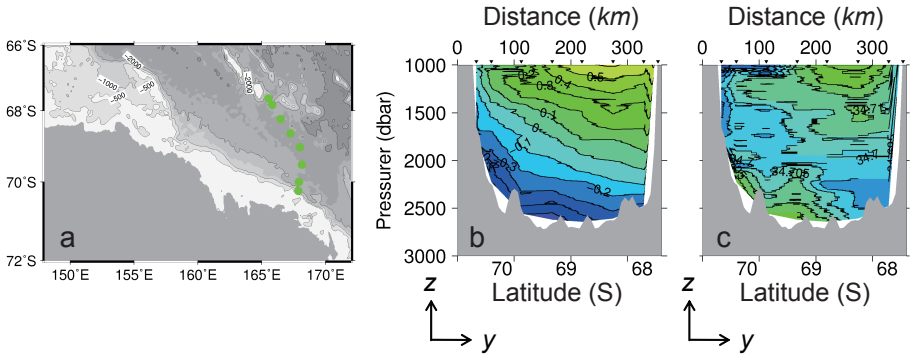

Fig. 7. Thickness and width (cross shore) of the RSBW from occupations in the 1990s. **(a)** Location of stations, **(b)** vertical cross section of potential temperature, **(c)** vertical cross section of salinity. *y* is cross shore coordinate (offshore positive), and *z* is vertical axis (upward positive). Thickness and width of cold and saline the RSBW are approximately 200 m and 200 km, respectively.

OSD
8, 2197–2235, 2011

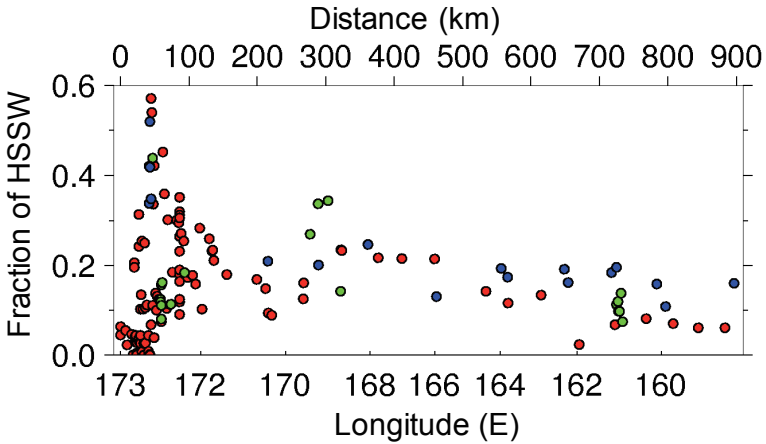

Fig. 8. Distribution of fraction of the HSSW within 100 m from bottom along flow path of the RSBW estimated by OMP analysis. Blue circles are from occupations in the 1970s, green circles are from 1990s and red circles are from 2000s.

OSD
8, 2197–2235, 2011

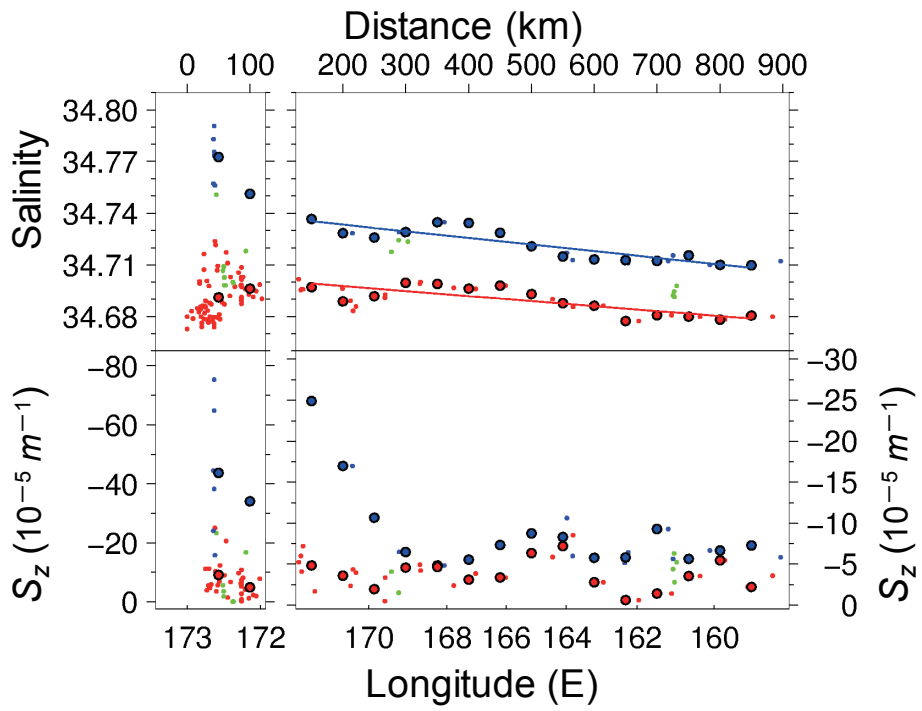

Fig. 9. Distribution of salinity averaged over the 100 m-thick layer at the bottom (upper panel) and vertical salinity gradient (lower panel) along flow path of the RSBW. Small circles are from occupations in the 1970s (blue), 1990s (green) and 2000s (red). In the estimation of vertical gradient, vertical gradients of 150 m scale are calculated at every 1 m interval by linear least square fit for each profile. The largest vertical gradients within 300 m from bottom are adopted as vertical gradient formed between the MSW/RSBW and the ambient water. Large circles are bin averages for the 1970s and 2000s and same colors as those for small circles are given. Solid lines in upper panel are regression lines for bin averages in region between 150 km and 900 km downstream from the Drygalski Trough.

OSD
8, 2197–2235, 2011

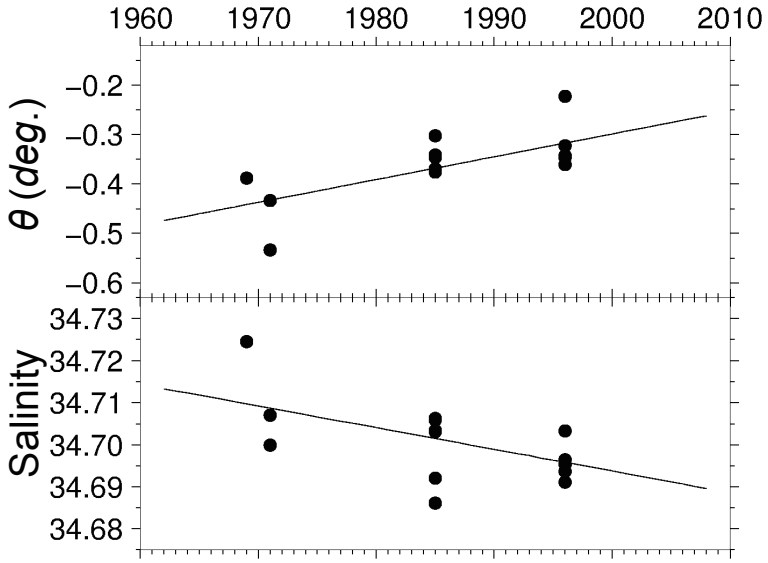

Fig. 10. Potential temperature (upper panel) and salinity (lower panel) averaged over the 100 m-thick layer at the bottom vs. year with regression lines from region around 150° E. Profiles locate within the box a in Fig. 6d are used here.

OSD
8, 2197–2235, 2011